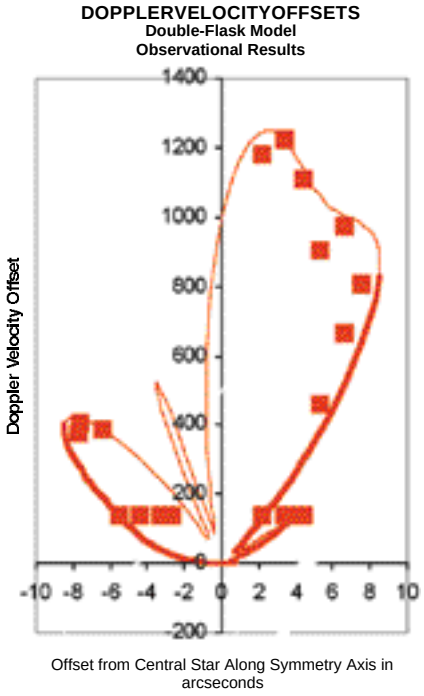

Figure 7: Velocity (in km s^{-1}) as a function of the distance to the central star, along the symmetry axis. Comparison of the Fabry-Perot Observations and the Double-Flask Model. The red line illustrates the predicted Doppler velocities for the Double-Flask Model for the locally reflected Brγ line. This uses the published parameters (with no adjustable parameters) for the Double-Flask model. The thick red line indicates that part of the Homunculus that can be seen by an observer. The red boxes are the observations of the Doppler velocities, that is, the spectral peaks found in the set of 8 curves similar to Figure 6, for each of 8 patches along the symmetry axis of the Homunculus in Figure 5 (2 peaks per spatial position, corresponding to the front and the back wall).

visible front wall that were derived from other data. In addition, for the first time, we can observe the structure and measure the velocities of the invisible back wall from the data obtained using the Fabry-Perot Interferometer and the coronographic spot of the ADONIS system.

Conclusion

We have verified that the assumption of rotational symmetry, which was made in the earlier analysis[3, 8] is indeed correct. These data also illustrate that the Double-Flask Model is strongly preferred over the Double-Sphere and the Double-Cap models. Finally, this analysis also confirms the orientation of the symmetry axis with respect to the line of sight of 40 ± 2 degrees. Further analysis will address the refinement of the Double-Flask parameters (rather than the discrimination between different models).

Acknowledgements

We wish to thank the 3.6-metre team at La Silla for support in the ADONIS observations.

References

[1]Currie, D.G. and D.M. Dowling. (1999) “Eta Carinae at the Millennium”, ASP Conference Series, Vol. 179, 1999, J.A. Morse, R.M. Humphries, and A. Damineli, eds.

[2]Currie D. G., D. M. Dowling, et. al., 1996, *AJ* **112**, 1115.

[3]Currie, D.G., D.M. Dowling, E. Shaya, J.J. Hester (1996), “Role of Dust in the Formation of Stars”, Garching bei München, Federal Republic of Germany, 11–14 September 1995. Proceedings of the ESO Workshop, Käufl, H. U. and Siebenmorgen, R. (Ed.) Springer-Verlag, 89–94.

[4]Allen, D.A. and D.J Hillier, 1993. Proc. Astron. Soc. Aust, **10** 338.

[5]Allen, D.A. and D.J Hillier, 1989, *MNRAS* **241**, 195–207.

[6]Currie, D., E. Diolaiti, S. Tordo, K. Naesgarde, J. Liwing, O. Bendinelli, G. Parmeggiani, L. Close, D. Bonaccini, 2000, SPIE, 4007-73.

[7]Dowling, D.M. (1996), “The Astrometric Expansion and 3-D Structure of eta Carinae” University of Maryland, Ph. D. Thesis.

[8]Meaburn, J., J.R. Walsh and R. D. Wolstencroft (1993), *A&A* **213** 89.

[9]Schulte-Ladbeck, R.E., A. Pasquali, M. Clampin, A. Nota, D.J. Hillier, O.L. Lupie (1999), *AJ* **118**, 1320.

[10]Currie, D. et al. 2000. *The Messenger* **100**, 12.

Unlocking the Past of Sakurai’s Object Using FORS/VLT

F. KERBER[1], R. PALSA[2], J. KÖPPEN[3,4,5], T. BLÖCKER[6], M.R. ROSA[1]

[1]Space Telescope European Coordinating Facility; [2]European Southern Observatory;
[3]Observatoire Astronomique, Strasbourg, France; [4]International Space University, Illkirch, France;
[5]Universität Kiel, Germany; [6]Max-Planck-Institut für Radioastronomie, Bonn, Germany

1. Summary

Sakurai’s object (V4334 Sgr) was discovered by Japanese amateur astronomer Y. Sakurai in February 1996 and first classified as a slow nova. Follow-up observations though immediately showed this to be a very special object indeed. It turned out to be a true stellar chameleon, perhaps the most rapidly evolving star ever witnessed. Details of its discovery and early observations are found in Duerbeck et al. (1996, 1997), Kerber et al. (1998) and Clayton & de Marco (1997). We have now used the combined power of FORS/VLT in order to deepen our insight into this object and its evolution.

Using FORS/VLT observations, we have obtained the best spectrum of the old PN surrounding Sakurai’s object. We have derived improved values for the interstellar reddening and we have been able to reliably measure additional diagnostic lines. In particular, the value found for the He II 4686 line is in excellent agreement with our earlier model calculations. We thereby confirm the previous result that the star was a hot, highly evolved PN nucleus before the flash.

2. The Nature of Sakurai’s Object

Today astronomers think that Sakurai’s object is undergoing a final helium flash. Helium (shell) flashes are common on the asymptotic giant branch (AGB) when stars burn hydrogen and helium intermittently. While hydrogen burning can be gradually turned on, helium ignites in a thermo-nuclear runaway leading to a very abrupt increase in brightness, hence the term flash or thermal pulse. As a consequence of this behaviour, stars lose a very significant percentage of their mass within a short period of time leaving only a thin atmospheric layer on top of the former stellar core when it leaves the AGB. The post-AGB star heats up while shrinking physically and therefore moves horizontally in the HRD. Upon reaching 30,000 K, the matter lost previously (AGB wind) gets ionised and becomes visible as a planetary nebula (PN). This PN central star will quickly (few 1000 to 10,000 years) exhaust the remaining hydrogen fuel and then en-

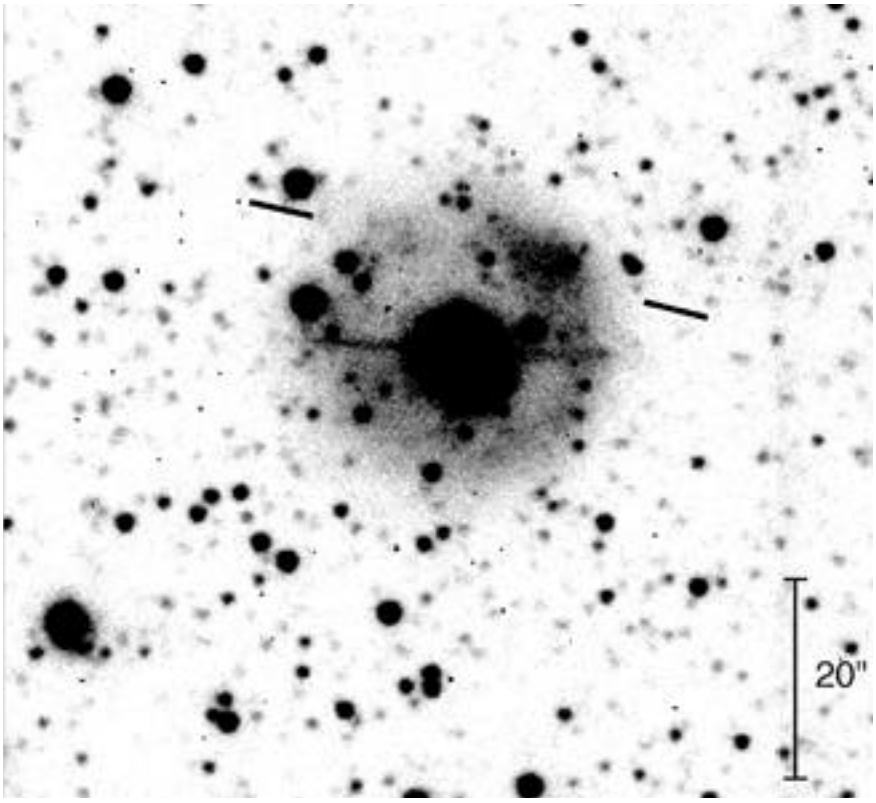

Figure 1: Hα image of the PN surrounding Sakurai's object. The slit position is indicated by the solid bars.

ters the white dwarf cooling track, while the PN quickly fades and mixes into the interstellar medium. Theory predicts though that for 10 to 20% of all low-mass stars one final, and delayed helium flash will occur with dramatic consequences: The renewed supply of energy balloons the star to giant dimensions, again sending it back to the AGB with a massive increase in brightness. The term born-again giant has been coined for such re-animated stars. The idea that Sakurai's object is indeed such a born-again giant is now based on several observational facts summarised below.

• The star is surrounded by a round nebula showing a spectrum typical for an evolved planetary nebula. This is strong evidence that the star must have been on the AGB previously and also had already evolved into a hot PN nucleus.

• V4334 Sgr's photosphere is highly deficient in hydrogen but enriched in heavier elements (Asplund et al. 1997, Kipper & Klochkova 1997). Furthermore, its composition has been found to change over time as hydrogen was further depleted, whereas s-process elements have increased in abundance (Asplund et al. 1999). This behaviour can be explained in terms of a very late helium flash during which the outer H-rich atmosphere is ingested into the helium burning shell while processed material from the stellar interior is mixed up to the surface resulting in the peculiar abundance pattern.

• The time evolution of the brightness is in general agreement with both the model (Iben et al. 1983) for a *very late* helium flash (i.e. after the end of H-burning, in contrast to a *late* flash which happens while H-burning is still active (suggested for FG Sge, by Blöcker & Schönberner 1997) and the other possible historic example for a very late helium flash, V605 Aql, the central star of A 58 (Seitter 1987).

• Another fact supporting the born-again hypothesis is the formation of molecular features (Asplund et al. 1997, Kerber et al. 1997) and of large amounts of hot dust as the star returns to the AGB. Our ISO observations covering four epochs over one year showed a tenfold increase in the 4 to 25 µm range (Kerber et al. 1999b). We found a significant mass-loss rate, which also appears to vary. During the same period the visual light curve went through a series of deep declines as the dust became optically thick. This behaviour is similar to R CrB stars, a rare class of irregular variable stars, which form clouds of dust close to the photosphere blocking our line of sight. A similar process seems likely for Sakurai's object.

3. The VLT Observations

One crucial piece of evidence would be to know about the properties of Sakurai's object before the helium flash. Such information is hard to come by directly as the only observations on record are Schmidt survey plates, which might just show it at the plates' limit of 21 mag in R. However, the density of the PN around the Sakurai's object is so low that it responds very slowly to the cut-off of UV photons, in fact, it will take hundreds of years to recombine. Therefore, the nebular plasma keeps a memory of the ionisation when the star was still hot enough to ionise it. With our VLT observation, we follow up earlier work by Pollacco (1999) and ourselves (Kerber et al. 1999a) in which we were able to confirm that Sakurai's object was indeed a highly evolved PN nucleus when the flash occurred.

The PN surrounding V4334 Sgr is an evolved round nebula of very low surface brightness which has a rather mottled appearance, and a brighter segment in the NW sector (Fig. 1). The angular diameter of 32 arcsec was given by Duerbeck & Benetti (1996). Jacoby et al. (1998) have clearly detected emission out to a diameter of 44 arcsec. In our 2D spectrum (Fig. 2) obtained with FORS 1 we can trace nebular emission to a maximum extent of about 39 arcsec. Since our slit only cuts through a section of the nebula, this is in agreement with the larger diameter reported.

As this is a photon-hungry enterprise, we decided to simply put to use the enormous light gathering capability of VLT's Antu in order to obtain a very deep spectrum of the PN. We therefore observed with FORS 1 using a single long slit on a single slit position that was centred on the brightest part of the nebula and covered a large fraction of the diameter but avoided V4334 Sgr itself, which was still a bright object at the time. No particular request in terms of seeing was made. The slit was 8 arcsec long and 2.5 arcsec wide. Specifically we aimed for a high signal-to-noise ratio and a large spectral coverage. To this end we used three different set-ups, Grism 300V (without filter), 300V with GG435 and Grism 300I with OG590. We had planned individual exposures of 2400 s each, which would then be combined during data reduction. Due to some technical problems, the observations were executed in a somewhat different manner, but that did not compromise their quality nor the scientific value. For 300V without filter, a total of 13,919 s were obtained in six exposures, for 300V+ GG435, 4800 s in two exposures, and for V300I+OG590 we integrated for 6961 s in four exposures, which gives a total integration time on the object of 25,680 s or just over seven hours in service mode.

A major part of the data reduction was performed using a developers release of the FORS pipeline software,

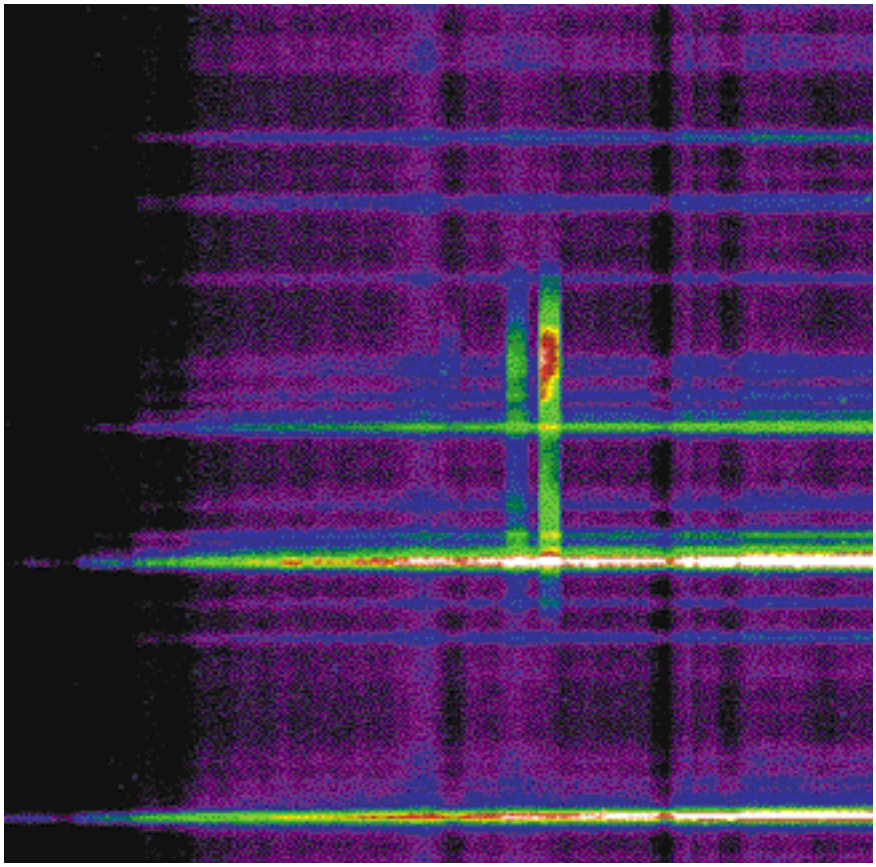

Figure 2: 2-D representation of a single FORS exposure with Grism 300V (2400 s). Shown is a region centred on 5000 Å with the two prominent [O III] lines. Slit width 2.5 arcsec.

which was made available to us by the Data Management and Operations Division (DMD) for evaluation. The FORS pipeline is implemented as a MIDAS context. In addition to the MIDAS package, we also had the chance to use the complete pipeline infrastructure (Data Organiser, Reduction Block Scheduler and Local Calibration Database) as it is used at the Paranal Observatory and by Data Flow Operations (DFO) in Garching. Usually, the pipeline infrastructure is not available to normal users. They have to use the MIDAS context RBS instead, which is part of the latest MIDAS release.

The pipeline was used to process the raw instrument calibration data (biases, flat fields) for each of the three instrument set-ups, which came bundled with the actual observations, to create master versions of the instrument calibration data. Also the dispersion relation was reliably determined by the pipeline for all instrument set-ups except for Grism 300I. It turned out that this was due to the emission-line catalogue used by the pipeline, which was not best suited for the combination of Grism 300I and 2.5 arcsec slit (a revision of the line catalogues used by the FORS pipeline is currently on its way). Therefore, a calibration-lamp exposure for the same instrument set-up, but for the FORS slit having a width of only 1.0 arcsec, was requested from the Science Archive for Grism 300I and processed by the pipeline. The obtained dispersion relation was then manually shifted by the appropriate offset which has been determined by cross correlating the line positions from the 2.5 arcsec slit exposure and the 1.0 arcsec slit exposure.

The science observations and the observations of the spectrophotometric standard stars were fed through the pipeline. As a final product we obtained linearly rebinned, 2-dimensional spectra for the science data and sky subtracted, optimal extracted spectra for the spectrophotometric standards. Processing of spectrophotometric standards is still under evaluation by DFO and therefore not routinely used for pipeline reduction of service-mode data, but the results obtained with the developer's version of the FORS pipeline available to us are well within the limits set by our requirements.

Figure 2 shows a section of the 2D spectrum after bias subtraction and flat fielding have been performed. The dominant features are the emission lines from the night sky, many of which are much stronger than the nebular emission. After visual inspection, the spectrum was extracted and special care was taken to avoid contamination from brighter stars in the crowded field.

4. Results

The spectrum of the PN around Sakurai's object we obtained with the combination of FORS/VLT has the highest S/N ever obtained. Furthermore, it extends the spectral coverage towards the red making additional lines available for analysis. From the Balmer decrement we derive a reddening E(BV) of 0.79, which is somewhat higher than earlier values derived from optical studies, but still within the error bars. This has some implications for the notoriously problematic distance determination. Highly discrepant values for the distance had been suggested by different methods (e.g. Duerbeck et al. 1997, Kimeswenger & Kerber 1998). The extinction distance method has yielded significantly lower values than other methods. With the new reddening value, distances larger than 2 kpc become possible and an improved reddening vs. distance relation is re-

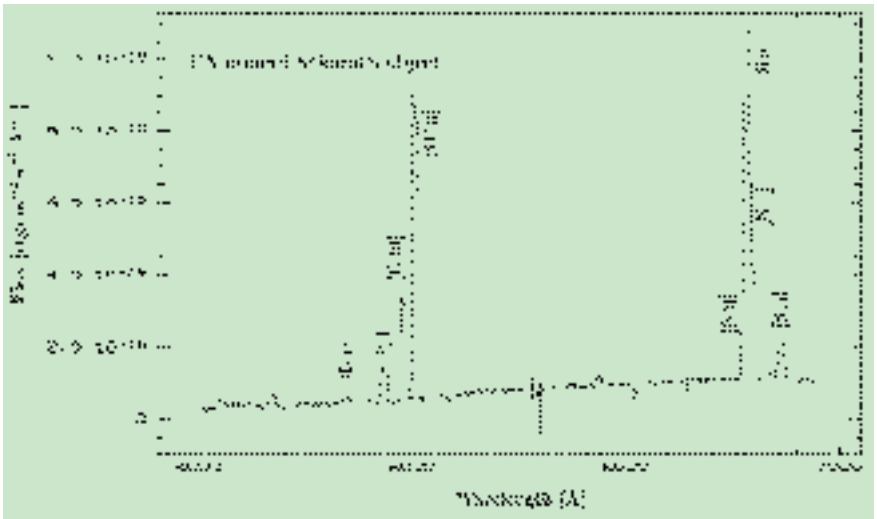

Figure 3: Spectrum extracted from a combination of the six Grism 300V exposures.

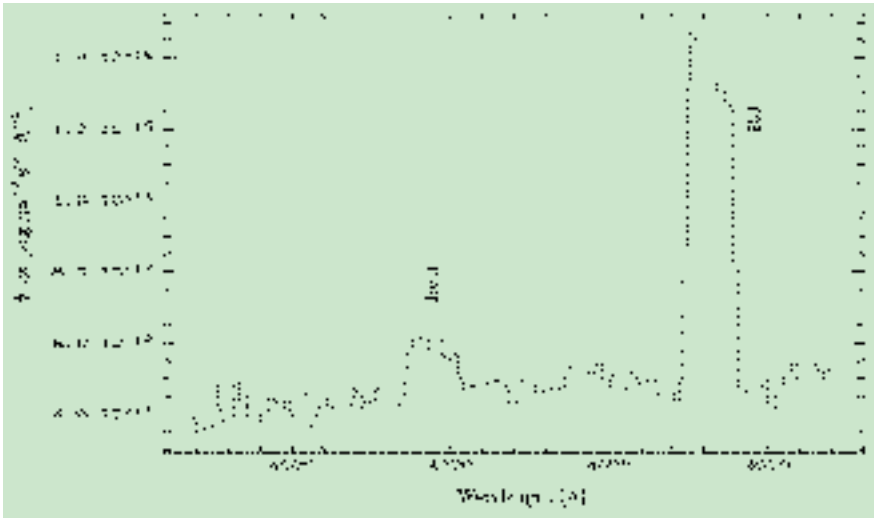

Figure 4: Expanded view of part of Figure 3 showing Hβ and the He II 4686 line.

Table 1: Intensities relative to I (Hβ) = 100, corrected with an extinction of c = 1.17.

λ [Å]	ID	*I/I* (Hβ)
4101	Hδ	27.23
4340	Hγ	58.5
4363	[O III]	5.9
4471	He I	9.2
4686	He II	19.0
4861	Hβ	100
4959	[O III]	280.0
5007	[O III]	857.5
5875	He I	8.8
6548	[N II]	48.6
6563	Hα	304.3
6583	[N II]	171.0
6678	He I	5.0
6717	[S II]	31.7
6731	[S II]	22.2
7135	[Ar III]	14.1
7750	[Ar III]	3.1
9069	[S III]	27.4
9531	[S III]	78.1

quired to finalise the distance. From the nebular spectrum and the appropriate ionisation models alone a constraint on *d* cannot be obtained. Thus a reliable and accurate distance remains the greatest obstacle to a better understanding of Sakurai's object.

Preliminary analysis of the VLT data shows that most of the findings reported earlier can now be confirmed with a much higher level of confidence. In particular the best ionisation model in our previous study predicted an He II 4686 flux of about 20% of Hβ. This is beautifully corroborated by the new observations which show the helium line at a strength of 19% of Hβ (Table 1 and Figs. 3 and 4).

In our previous model we had assumed solar chemical composition, for which we had obtained a rather good fit. It has been demonstrated before that nebulae around hydrogen-deficient central stars have perfectly normal abundances. Examples are K 1-27 and LoTr 4 (Rauch et al. 1994, 1996).

With the photoionisation code GWYN (Köppen 1979; Rauch et al. 1996) we computed a grid of spherically symmetric models of solar composition nebulae, all having an angular diameter of 32 arcsec at a distance of 1.5 kpc, with a density of 100 cm^{-3}. The best fit is given by $T_* = 98{,}000 \pm 7000$ K and $L_* = 25 \pm 5\ L_\odot$. For a distance of 5.5 kpc the best fit is at $T_* = 95{,}000 \pm 7000$ K and $L_* = 240 \pm 40\ L_\odot$. Our results show that Sakurai's pre-flash position in the HRD was indeed that of a highly evolved PN central star, entering the white dwarf cooling tracks. Thus, it is truly a case of a very late helium flash.

References

Asplund, M., Gustafsson, B., Lambert, D.L., Kameswara Rao, N., 1997, *A&A* **321**, L 17.

Asplund, M., Lambert, D.L., Kipper, T., Pollacco, D., Shetrone, M.D., 1999, *A&A* **343**, 507.

Blöcker, T., Schönberner D., 1997, *A&A* **423**, 991.

Clayton, G.C., de Marco, O., 1997, *AJ* **114**, 2679.

Duerbeck, H.W., Benetti, S., 1996, *ApJ* **468**, L111.

Duerbeck, H.W., Benetti, S., Gautschy, A., van Genderen, A.M., Kemper, C., Liller, W., Thomas, T., 1997, *AJ* **114**, 1657.

Iben, I., Kaler, J.B., Truran, J.W., Renzini, A., 1983, *ApJ* **265**, 605.

Jacoby, G.H., de Marco, O., Swayer, D.G., 1998a, *AJ* **116**, 1367.

Kerber F., Gratl H., Roth M., 1997, IAU Circ. 6601.

Kerber, F., Gratl, H., Kimeswenger, S., Roth, M., 1998, *Ap&SS* **255**, 279.

Kerber, F., Blommaert, J.D.A.L., Groenewegen, M.A.T., Kimeswenger S., Käufl, H.-U., Asplund M., 1999a, *A&A* **350**, L27.

Kerber F., Köppen J., Roth M., Trager S.C., 1999b, *A&A* **344**, L 79.

Kimeswenger, S., Kerber, F., 1998, *A&A* **330**, L 41.

Kipper, T., Klochkova, V.G., 1997, *A&A* **324**, L 65.

Köppen, J., 1979, *A&AS* **35**, 111.

Pollacco, D., 1999, *MNRAS* **304**, 127.

Rauch, T., Köppen, J., Werner, K., 1994, *A&A* **286**, 543.

Rauch, T., Köppen, J., Werner, K., 1996, *A&A* **310**, 613.

Seitter, W.C., 1987, *The Messenger* **50**, 14.

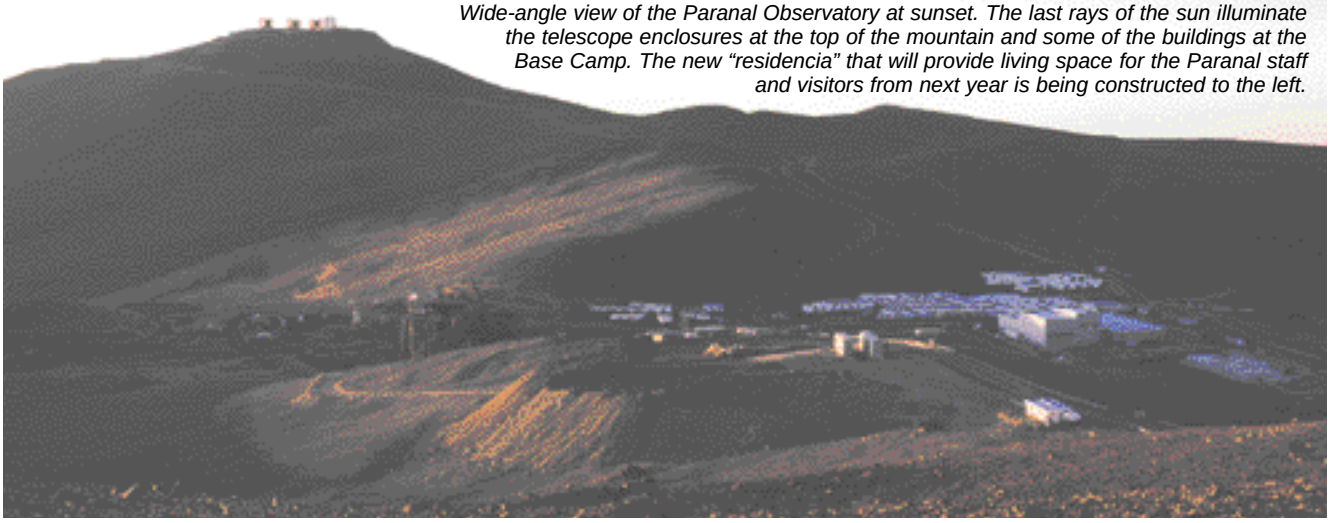

Wide-angle view of the Paranal Observatory at sunset. The last rays of the sun illuminate the telescope enclosures at the top of the mountain and some of the buildings at the Base Camp. The new "residencia" that will provide living space for the Paranal staff and visitors from next year is being constructed to the left.